

Figures from ch. 9 of *Photonic Crystals*

Steven G. Johnson, MIT course 18.369

May 3, 2010

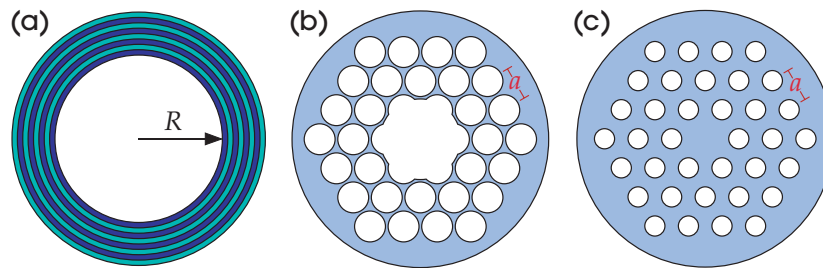


Figure 1: Three examples of photonic-crystal fibers. (a) Bragg fiber, with a one-dimensionally periodic cladding of concentric layers. (b) Two-dimensionally periodic structure (a triangular lattice of air holes, or “holey fiber”), confining light in a hollow core by a band gap. (c) Holey fiber that confines light in a solid core by index guiding.

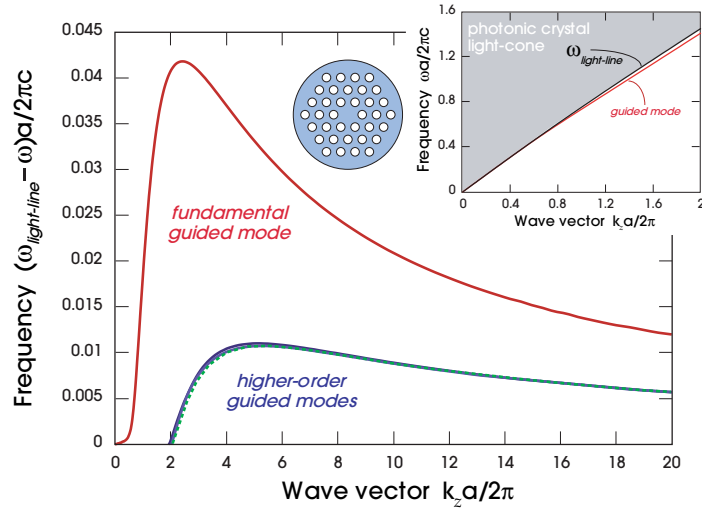


Figure 2: Band diagram of solid-core holey fiber as a function of axial wave vector k_z . The usual ω plot is inset, but for clarity we also plot the $\Delta\omega$ between the guided bands and the light line. The higher-order guided modes are three bands that are nearly on top of one another.

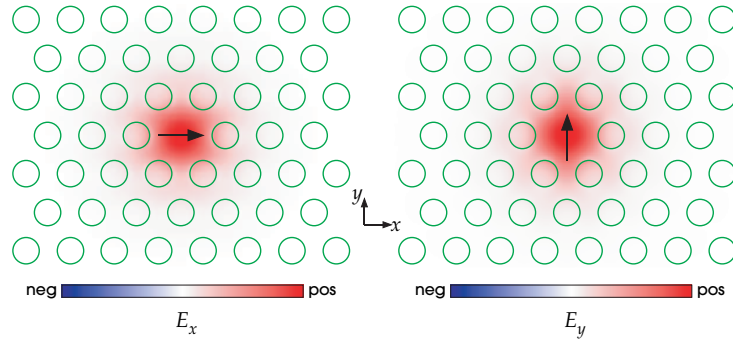


Figure 3: Electric-field pattern for the doubly degenerate fundamental mode of figure 2. Their polarizations are nearly orthogonal everywhere: the mode pictured at left is mostly E_x , and the mode pictured at right is mostly E_y . The green circles show the locations of the air holes.

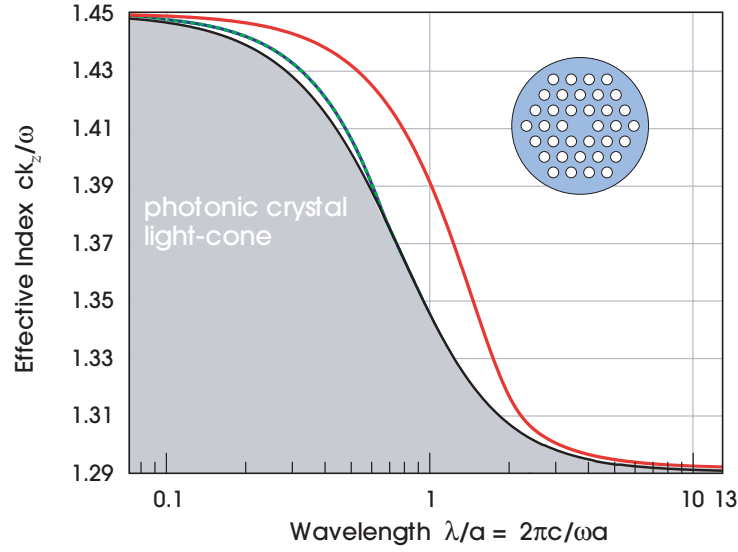


Figure 4: Bands of the solid-core holey fiber, from figure 2, plotted as “effective index” ck_z/ω versus wavelength, along with the light cone (gray region). In the limit of small λ , the effective indices of both the modes and the light line approach the index 1.45 of the bulk silica.

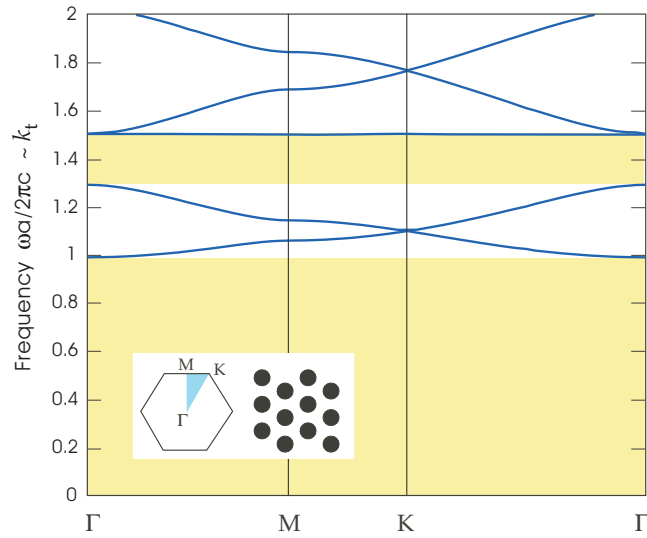


Figure 5: Band diagram for TM-polarized modes of a two-dimensional triangular lattice of perfect-metal cylinders. Two band gaps are shown (shaded yellow), where the lowest band has a low-frequency cutoff characteristic of metallic structures. These bands are equivalent to the modes of the holey fiber in the scalar (large k_z) limit.

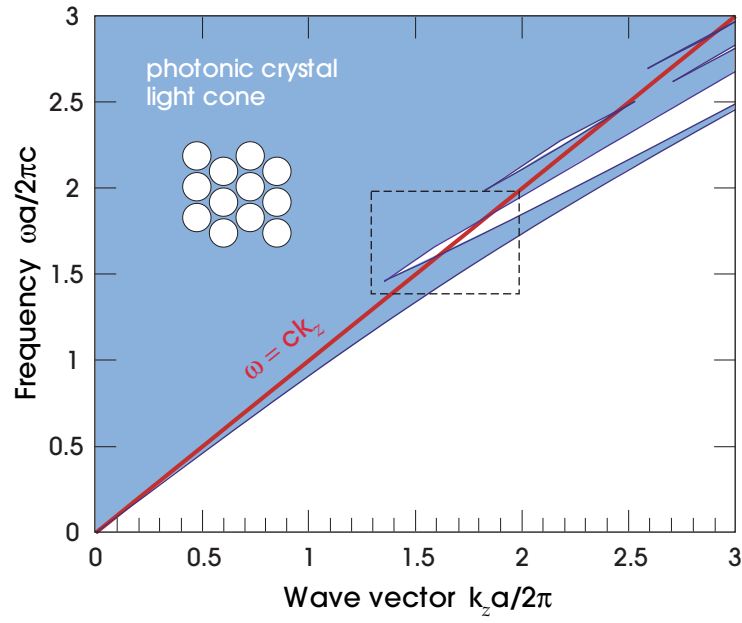


Figure 6: Projected band diagram, as a function of out-of-plane wave vector k_z , for a triangular lattice of air holes (inset: period a , radius $0.47a$) in $\epsilon = 2.1$. This forms the light cone of the holey fiber from figure 1(b), with gaps appearing as open regions. The light line of air, $\omega = ck_z$, is shown in red. (Dashed box indicates region plotted in figures 9 and 11 for the defect modes.)

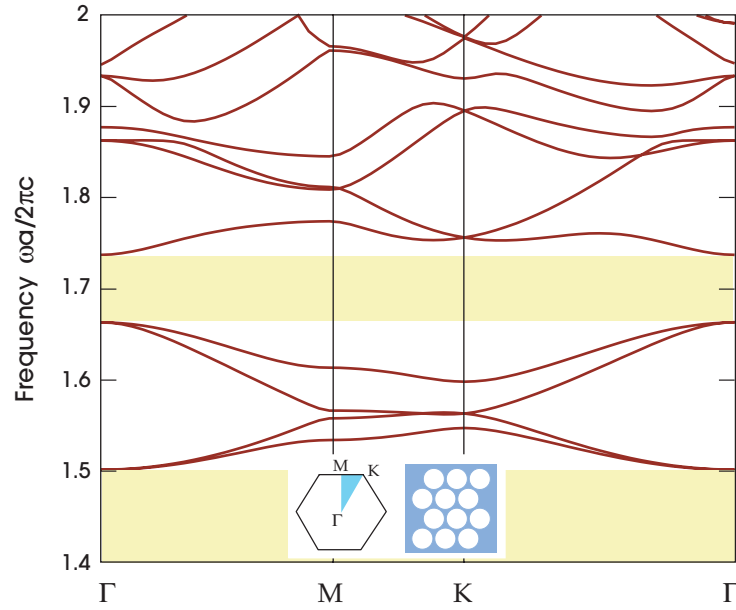


Figure 7: Band diagram versus in-plane wave vector in the irreducible Brillouin zone (inset) for the triangular lattice of air holes from figure 6, at an out-of-plane wave vector $k_z a/2\pi = 1.7$. Gaps are shaded yellow: the lower gap corresponds to the index-guiding region, and the upper gap corresponds to one of the band gaps inside the light cone where guiding in an air core is possible.

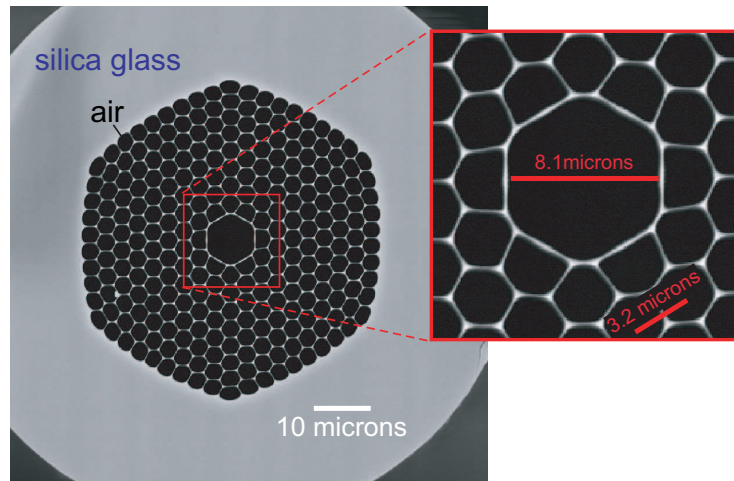


Figure 8: Electron-microscope image of hollow-core holey-fiber cross section (black regions are air holes, and gray regions are silica glass). Central air defect, replacing 7 holes, supports gap-guided modes around a wavelength of 1060 nm. (Image courtesy Karl Koch and Corning, Inc.)

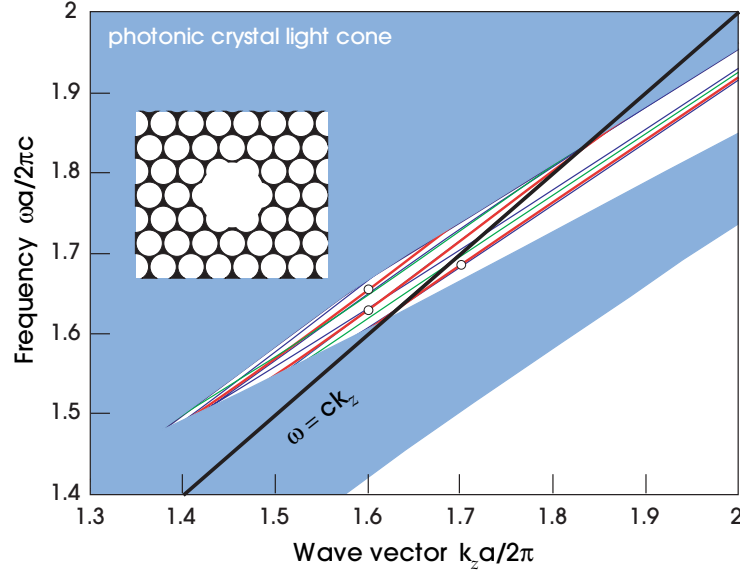


Figure 9: Band diagram showing guided modes of hollow-core holey-fiber structure (inset, similar to experimental structure of figure 8), corresponding to dashed region of figure 6. (Air core is formed by a radius-1.202a air hole.) Three thick red lines indicate doubly degenerate bands that have the correct symmetry to couple to planewave input light. Thin green lines indicate doubly degenerate bands with a different symmetry, and thin blue lines indicate nondegenerate bands. Bands below the light line (thick black) are surface states confined to the edge of the core. Three dots indicate the modes plotted in figure 10.

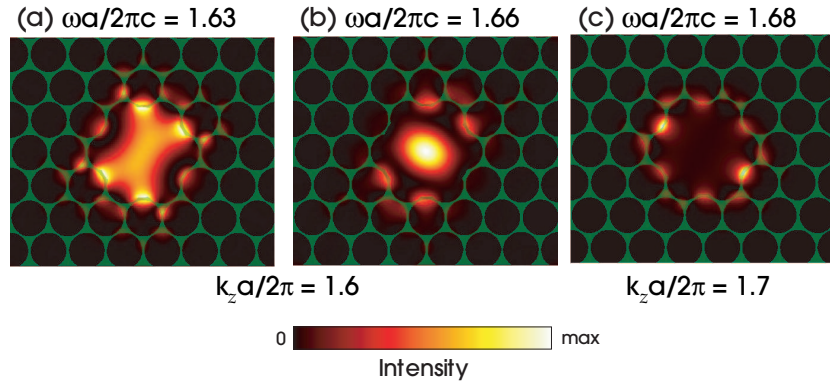


Figure 10: Intensity patterns ($\hat{\mathbf{z}} \cdot \text{Re}[\mathbf{E}^* \times \mathbf{H}]$) of three doubly degenerate modes of a hollow-core holey fiber (ϵ shaded green), corresponding to the dots on the thick red lines in figure 9. (a) and (b) lie above the air light line at $k_z a/2\pi = 1.6$, while (c) is a surface state lying below the air light line at $k_z a/2\pi = 1.7$.

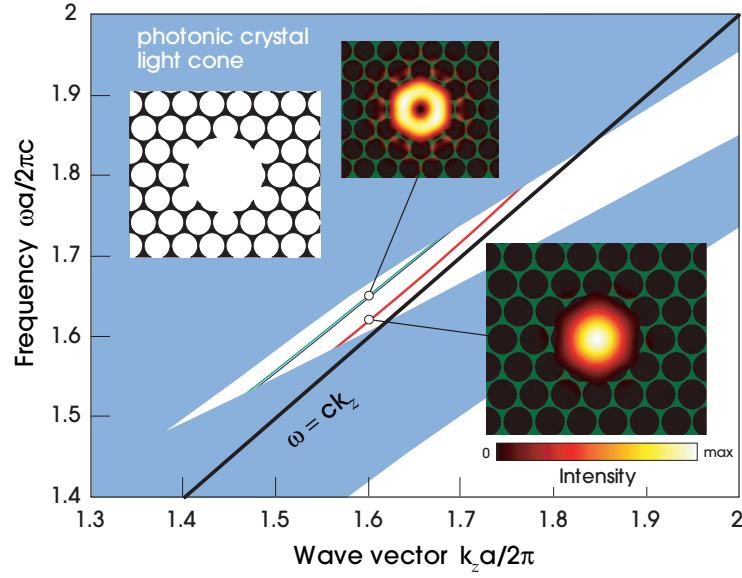


Figure 11: Band diagram and mode intensity patterns (insets) of a hollow-core holey fiber with a larger air core (radius $1.4a$, left inset) corresponding to a crystal termination that eliminates surface states. Thick red line (lower) indicates doubly degenerate mode with correct symmetry to couple to input plane waves. Thin blue and green lines indicate other symmetries (blue is nondegenerate and green is doubly degenerate); there are actually two blue lines that are difficult to distinguish here. Intensity patterns are shown for $k_z a/2\pi = 1.6$, indicated by the dots. (The four higher-order modes all have similar intensity patterns; a nondegenerate mode is shown.)

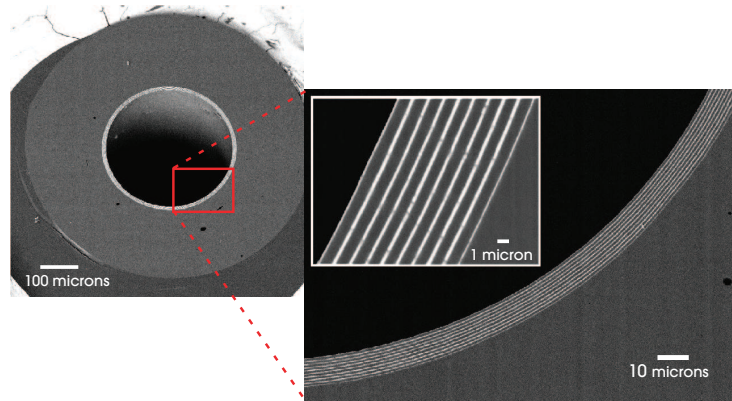


Figure 12: Electron-microscope image of a hollow-core omnidirectional-mirror Bragg-fiber cross section, with insets showing enlarged views of multilayer structures. Thin white layers are a chalcogenide glass and gray regions are a polymer. This fiber was designed to operate at a wavelength of $10.6 \mu\text{m}$ (?).

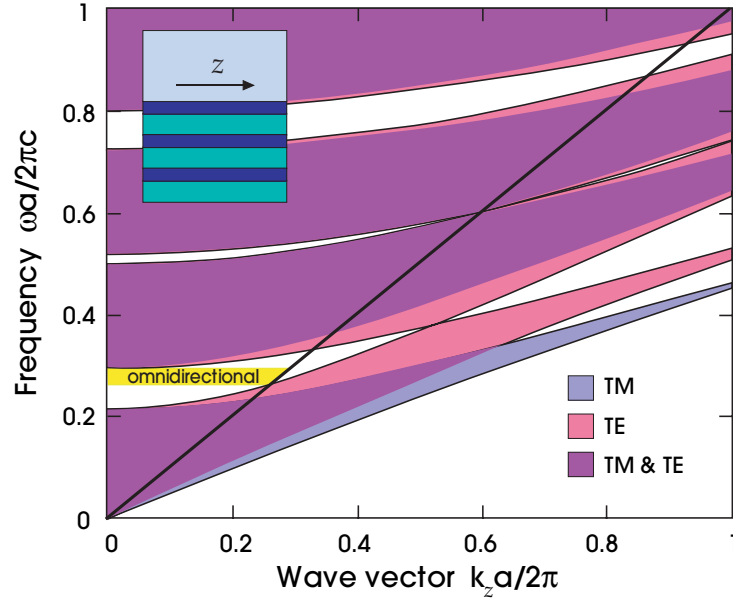


Figure 13: Projected band diagram for glancing-angle quarter-wave stack of indices $n_1 = 1.6$ and $n_2 = 2.7$, plotted versus wave vector k_z parallel to layers (inset). Regions where propagating modes exist in the stack are shaded: blue for TM (\mathbf{E} out of the incidence plane) and red for TE (\mathbf{E} in the incidence plane), or purple for both. The frequency range of omnidirectional reflection from an air medium (corresponding to the black light line $\omega = ck_z$) is shaded yellow. (Note that this “TM/TE” terminology is the reverse of the “te/tm” terminology used later in the chapter.)

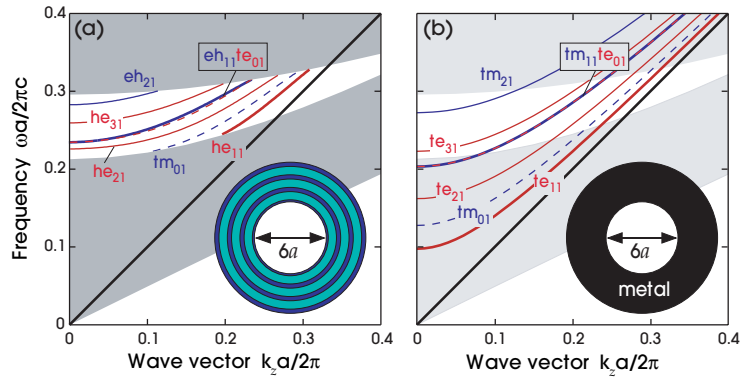


Figure 14: (a) Band diagram of hollow-core ($R = 3a$) Bragg fiber with layer indices of 2.7/1.6 (blue/green layers in inset); gray regions indicate extended modes that propagate in the multilayer mirrors. (b) Band diagram showing the first few bands of a hollow perfect-metal waveguide of the same radius; light gray regions indicate extended modes of Bragg mirrors from (a), for comparison. Modes are labelled by polarization and radial/angular mode numbers as described in the text.

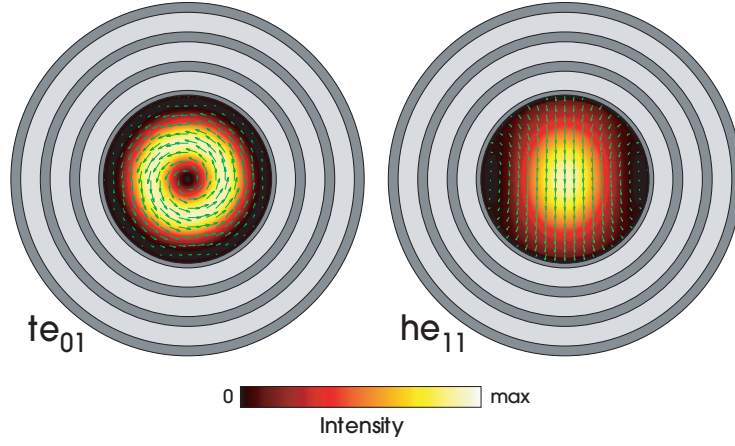


Figure 15: Intensity patterns for two core-guided modes in hollow-core Bragg fiber of figure 14 at the quarter-wave frequency. Power intensity is shown by color scale, and transverse (x,y) electric-field pattern is shown by green arrows.

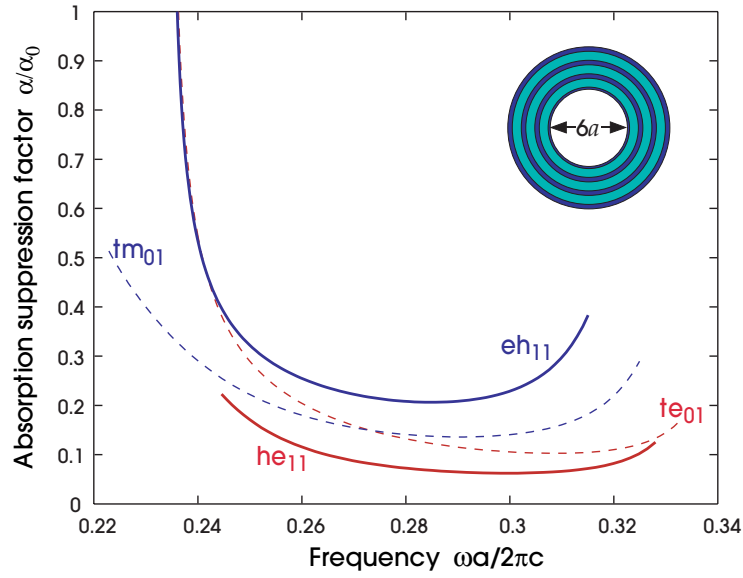


Figure 16: Absorption suppression factor α/α_0 of $R = 3a$ Bragg fiber from figure 14(a) versus frequency for four modes. α/α_0 is the ratio of the modes absorption losses to the absorption losses for the bulk material, assuming that the absorption losses are dominated by those of the low-index material ($n = 1.6$, shaded green in inset). Here, the he_{11} (fundamental) mode is the lowest loss, while for larger R the te_{01} mode becomes the lowest.

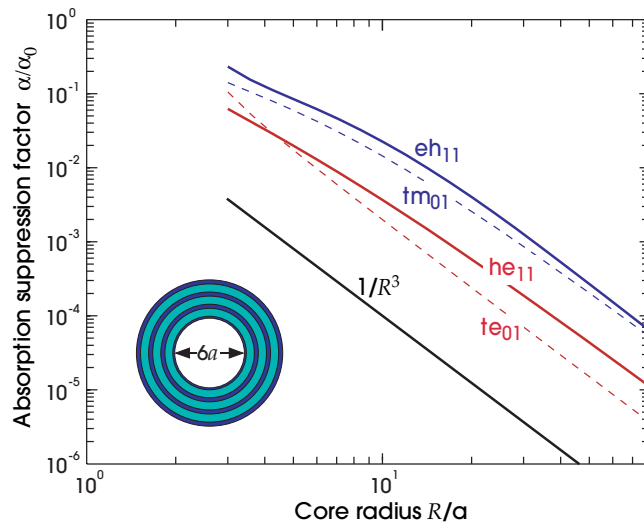


Figure 17: Scaling of the absorption suppression factor α/α_0 versus core radius R , at quarter-wave frequency, for several modes of the hollow-core Bragg fiber with indices 2.7/1.6 (blue/green in inset). The absorption loss is assumed to be dominated by that of the low-index material. All modes asymptote to a $1/R^3$ scaling (shown as a black line, for reference).